Dalton Transactions

ROYAL SOCIETY OF CHEMISTRY

PAPER

View Article Online
View Journal | View Issue

Cite this: *Dalton Trans.*, 2023, **52**, 6685

The π-interactions of ammonia ligands evaluated by *ab initio* ligand field theory†

Moritz Buchhorn and Vera Krewald *

Received 17th February 2023,
Accepted 7th April 2023

DOI: 10.1039/d3dt00511a

rsc.li/dalton

Ammonia and amine ligands are commonly assumed to be σ-only ligands in coordination chemistry, *i.e.* they are not expected to interact significantly with a metal *via* a π path. Ligand field analyses employing the Angular Overlap Model resulted in good fits to experimental data without a π parameter for ammonia ligands, thereby supporting this assumption. In this work, we challenge this assumption and suggest that it is an oversimplification. We use complete active space calculations for electronic structure analyses of copper ammine complexes that are in good agreement with the transitions observed in experimental UV-vis spectra. These findings lead to a reinterpretation of the experimental spectra that necessitates a significant π interaction of the ammonia ligands. The strength of the ammonia π interaction is evaluated by parameterizing the ligand field splittings of a series of metal hexammine complexes $[M(NH_3)_6]^{n+}$ with M = Cr, Mn, Fe, Co, Ni, Ru, Os and n = 2, 3) and selected tetrammine complexes $[M(NH_3)_4]^{n+}$ with M = Cr, Mn, Fe, Co, Ni and n = 2 or 3) with the Angular Overlap Model. The resulting π parameters show that ammonia is a π donor of similar strength as chloride.

Introduction

In coordination chemistry, it is frequently assumed that the interaction between a metal centre and an ammonia ligand is characterised exclusively by σ character and thus that any π character is negligible.[1–12] This can be rationalized in an orbital picture: ammonia does not have any molecular orbitals of π character; only the σ/σ* molecular orbitals of the N–H bonds are partly oriented such that the metal-ammonia binding axis can lie in the nodal plane of a metal d orbital. Ammonia is therefore commonly classified as a σ-only ligand.

Metal–ligand interactions can be evaluated with ligand field theory. Besides global ligand field descriptors like the ligand field splitting Δ or Racah parameters, the Angular Overlap Model (AOM) provides a ligand-specific parameterisation that conforms to the familiar interpretation of chemistry in terms of functional groups. The AOM quantifies the metal–ligand interaction *via* σ and π overlaps, with an additional parameter for d–s mixing.[2,13,14] The destabilisation of each pure metal d orbital with respect to the situation in the free ion is associated with a spherical component E and a directional component that is expressed with a specific number and magnitude of e_σ and e_π parameters depending on the coordination environment, see Fig. 1. The orbital splitting of tetrahedral and octahedral coordination spheres does not allow for a distinction between e_σ and e_π.[15] This means that neglecting e_π comes with the convenience of having an unambiguous relationship between e_σ and Δ. Lower symmetry coordination environments result in fewer orbital degeneracies which should provide a sufficient number of states to fit e_σ and e_π parameters simultaneously.

We recently developed an AOM parameter fitting procedure[16] based on *ab initio* ligand field theory[17–19] as a tool that provides insights into metal–ligand bonding situations. Notably, it is able to obtain AOM parameters for complexes for which previously the ligand field equation system would have been underdetermined. We showed that the method yields qualitatively correct parameters and reproduces expected chemical trends like the e_λ values of halide ligands being associated with their donor capacity and position in the spectrochemical series.[16]

In this paper, we present some incentives to rethink the assumption of amines being σ-only ligands. Firstly, we revisit the experimental UV-vis spectra of a square planar copper tetrammine and a pyramidal copper pentammine complex. They had been interpreted to not contain d–d transitions that would be expected if π interactions were present.[5] Their analysis with *ab initio* ligand field theory calculations demonstrates the need for an ammine π interaction. Building on this, we present and discuss AOM parameters for a series of octahedral and tetrahedral ammine complexes obtained with our recently presented AOM parameter fitting procedure.[16] We find that ammonia should be viewed as capable of significant π inter-

TU Darmstadt, Department of Chemistry, Theoretical Chemistry, Alarich-Weiss-Straße 4, 64287 Darmstadt, Germany. E-mail: vera.krewald@tu-darmstadt.de

† Electronic supplementary information (ESI) available. See DOI: https://doi.org/10.1039/d3dt00511a

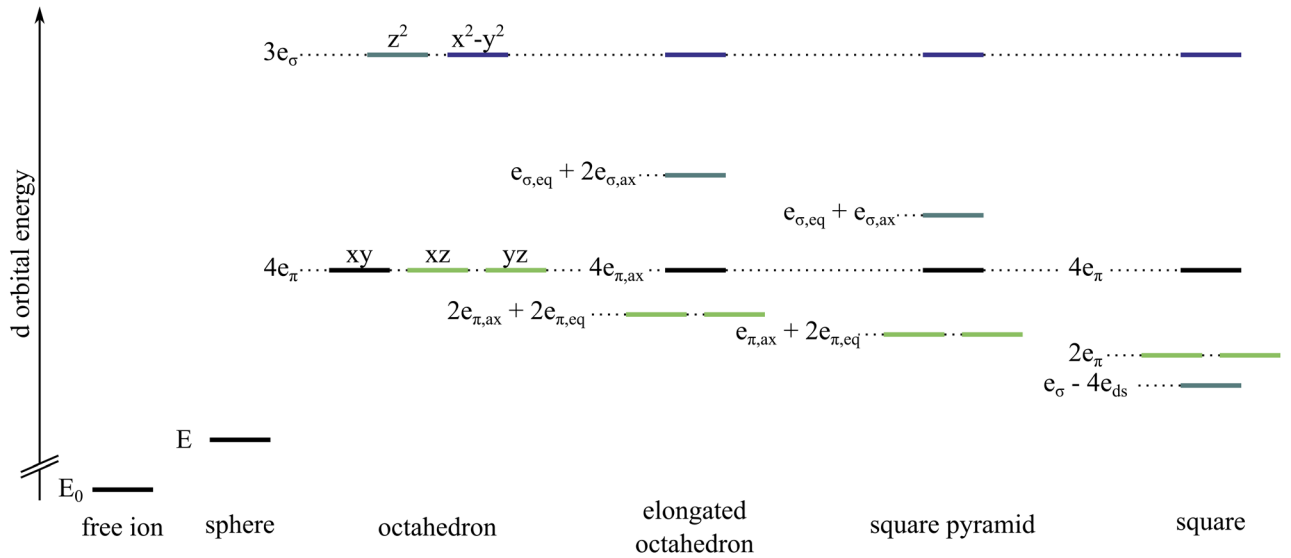

Fig. 1 Comparison of d orbital energy splittings for a free ion, a spherical potential and different coordination environments with the respective AOM parameters e_λ. The orbital levels are coloured as follows, d_{z^2} teal, $d_{x^2-y^2}$ dark blue, d_{xy} black, d_{xz} and d_{yz} light green. For an elongated octahedron and a square pyramid, the ligands on the *z*-axis have parameters labelled ax, while the others in the *xy*-plane are labelled eq. For symmetries with at least one d orbital in the totally symmetric representation, d–s mixing must be considered which affects the orbital energy by an additional parameter e_{ds}. More details regarding d–s mixing are provided in the ESI.†

actions (ranging from about 400 cm^{-1} to more than 1000 cm^{-1}), which raises the question of whether a true σ-only ligand can exist.

Methodology and computational details

The ORCA 4.2.1 quantum chemistry package[20,21] was used for all quantum chemical calculations. Geometries were optimized using the unrestricted Kohn–Sham formalism with the BP86 functional,[22,23] the def2-SVP basis set,[24] and the def2/J auxiliary basis.[25] The resolution of identity approximation for the Coulomb term was used.[26,27] Convergence criteria were NormalSCF for all self-consistent field calculations and TightOpt for geometry optimizations. The geometry optimizations employed the default integration grid (Accuracy 2: Lebedev 110 points) for optimization steps and the final SCF at the optimized geometry (Accuracy 4: Lebedev 302 points). Geometry optimizations of halide complexes of the type $[MX_6]^{3-/4-}$ with large negative charges additionally employed the CPCM/SMD solvation model with the parameters of water and an increased solvent radius of 3.0 Å to aid convergence.[28,29]

For square planar $[Cu(NH_3)_4]^{2+}$ and square pyramidal $[Cu(NH_3)_5]^{2+}$, the heavy atom positions were taken from the crystal structures (ICSD entries 14372 and 201229) and only the hydrogen atom positions were optimised with the settings stated above, but without employing a solvent model. The electronic states corresponding to the d orbitals were calculated using CASSCF[30,31] in the *ab initio* ligand field theory variant[17–19] with the def2-TZVP basis set. The calculations on $[Cu(NH_3)_4]^{2+}$ and $[Cu(NH_3)_5]^{2+}$ also employed a subsequent perturbation theory treatment (NEVPT2).[32–35] The active space was chosen to contain the five valence d orbitals and *n* d electrons, or in shorthand notation a CAS(*n*,5) space. The *ab initio* ligand field theory module[17] was employed to construct the effective ligand field Hamiltonian from the calculated states. For selected examples, spin–orbit coupling was considered using the spin–orbit mean field approach as implemented in ORCA.[36]

The AOM was used to fit the one-electron part of the ligand field Hamiltonian[13,37] according to our fitting procedure.[16] The ligand field matrix contains up to 15 unique equations, which quickly results in underdetermined problems. For instance for six-coordinate complexes, one needs to fit 13 parameters of the ligand field potential: *E*, six e_σ and six e_π. Such a fit is in theory possible but in practice, linear dependencies can occur in the equation system so that the actual number of equations can be lower than 13, resulting in an underdetermined problem.

We address this restriction by grouping chemically equivalent ligands at similar bond lengths (*e.g.* in Jahn–Teller distorted $[Mn(NH_3)_6]^{3+}$, ligands are grouped into axial and equatorial parameter sets). In practice, grouping is achieved by adding additional equations to the system that require $0 = e_{\sigma,L} - e_{\sigma,L'}$. From a formal perspective, one could use these equations to require parameters to be strictly equal and thereby reduce their number. For solving the least squares problem of the overdetermined system, the addition of more equations has different consequences than the reduction of the number of parameters. Additional equations allow the

parameters $e_{\sigma,L}$ and $e_{\sigma,L'}$ to deviate, even if they are expected to be equal. This flexibility is important, since the asymmetric distortions generated during the fitting procedure render the ligands not perfectly equivalent so that small deviations are expected. If not stated otherwise, all ligands in the complexes studied are put into a single group. Complexes with significant differences in bond lengths due to Jahn–Teller distortions have two or more ligand groups as indicated by labels.

Results

Pyramidal copper pentammine

An explicit assessment of π interactions is only possible for symmetries lower than O_h or T_d, see Fig. 1. The $[Cu^{II}(NH_3)_5]^{2+}$ subunit in $K[Cu(NH_3)_5][PF_6]_3$ [38] and $NH_4[Cu(NH_3)_5][PF_6]_3$ [39] is approximately square pyramidal (point group: C_{2v}) and thus represents a suitable test case. Another convenient feature is its d^9 electronic configuration that results in four d–d transitions. The interelectronic repulsion within each electronic state is equal, and therefore the energy differences of these states can be equated with the energy differences of the d orbitals.

The electronic spectrum of $[Cu(NH_3)_5]^{2+}$ (see Fig. 2a) shows a band at 15 300 cm^{-1} with a weak shoulder at 14 000 cm^{-1} and a second band at 11 000 cm^{-1}, see Table 1. The shoulder is assigned to a $d_{xy} \rightarrow d_{x^2-y^2}$ transition by Duggan *et al.*,[38] implying a state splitting of 1300 cm^{-1}. Within the AOM, this splitting results in an e_π value of 1300 cm^{-1} in a perfect square pyramid or even a slightly larger value in a C_{2v} distorted square pyramid (see ESI† for details). Since the shoulder is not a very pronounced feature, the signal was interpreted later as "essentially unsplit", ruling out a π interaction.[5] With this interpretation, ammonia is viewed as a σ-only ligand. This assumption was also made for other complexes.[6–12,40]

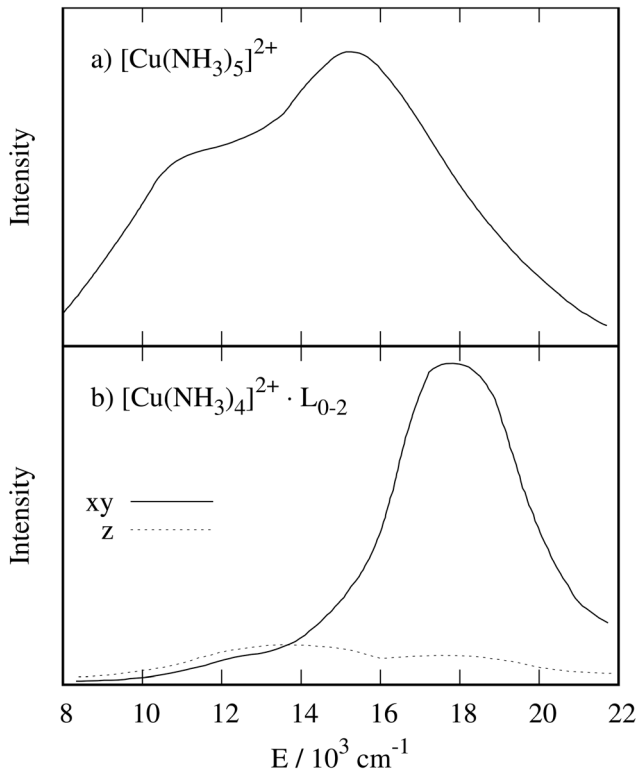

Fig. 2 Electronic spectrum of (a) $NH_4[Cu(NH_3)_5][PF_6]_3$, reprint from ref. 38 with permission from the Royal Society of Chemistry. Polarized electronic spectrum of (b) $Na_4[Cu^{II}(NH_3)_4{\cdot}L][Cu^{I}(S_2O_3)_2]_2$, reprint from ref. 41 with permission from the Royal Society of Chemistry. Please note the structural uncertainty of (b) discussed in the main text.

Table 1 Energies of the experimental and calculated d–d transitions for $[Cu(NH_3)_5]^{2+}$

	$d_{xz},d_{yz} \rightarrow d_{x^2-y^2}$/ cm^{-1}	$d_{xy} \rightarrow d_{x^2-y^2}$/ cm^{-1}	$d_{z^2} \rightarrow d_{x^2-y^2}$/ cm^{-1}
CASSCF	11 549–11 673	10 523	8 635
NEVPT2	16 145–16 308	15 341	11 687
Exp.	15 300	*ca.* 14 000	11 000

CASSCF/NEVPT2 calculations on the $[Cu(NH_3)_5]^{2+}$ subunit from the crystal structure yield an orbital ordering and d–d transitions in very good agreement with the measured ones, see Table 1. We note that while spin–orbit coupling (SOC) may be of importance for copper complexes (single-electron SOC parameter of *ca.* 830 cm^{-1} for free Cu^{2+}),[15] inclusion of SOC does not qualitatively alter the picture, see ESI.† The calculations thus fully support the spectral assignments of Duggan *et al.*, and hence the need for an ammonia π interaction of about 1300 cm^{-1}.

Square planar copper tetrammine

As a second example, we selected the $[Cu^{II}(NH_3)_4]^{2+}$ subunit in the crystal structure of $Na_4[Cu^{II}(NH_3)_4][Cu^{I}(S_2O_3)_2]_2$.[42] While initially, the crystal structure was thought to contain copper ions in a square-planar environment,[42] later studies suggested that one or two axial ammonia ligands may weakly coordinate.[43] Although the precise structure is therefore not clear, there are two independently reported UV-vis spectra.[41,44] Tomlinson *et al.* assigned the d–d transitions for the presumed square-planer complex using polarised electronic spectra, see Fig. 2b, leading to a one-electron orbital sequence of $d_{x^2-y^2} > d_{z^2} > d_{xy} \geq d_{xz},d_{yz}$.[41]

To evaluate the electronic structure with CASSCF/NEVPT2 calculations as for the square-pyramidal system, hydrogen atoms were added to complete the ammonia ligands of the $[Cu(NH_3)_4]^{2+}$ subunit and their positions were optimized (see computational details). The influence of one or two axial ammonia ligands was evaluated explicitly, see below. Using CASSCF calculations that facilitate a direct assignment of configurations to states, we arrive at a different energetic ordering for the square planar complex, namely $d_{x^2-y^2} > d_{xy} > d_{xz}$, $d_{yz} \approx d_{z^2}$ in agreement with other computational studies.[45–47] Giner *et al.* found this orbital ordering, notably including the pronounced energy difference between the d_{xy} and d_{xz}, d_{yz} levels, at different levels of theory that capture electron correlation

adequately, *e.g.* CCSD(T).[47] Atanasov *et al.* assigned an e_π of roughly 1200 cm^{-1} to NH_3 from an *ab initio* ligand field theory analysis.[48]

There is some uncertainty surrounding the exact composition of the ligand field experienced by the copper ion in the crystal structure,[42,43] where the gaps between the square planar $[Cu(NH_3)_4]^{2+}$ subunits are large enough to host ammonia molecules. These additional molecules would result in axial Cu–N distances of 2.88 Å. We investigated these different possibilities with one or two ammonia ligands approaching the copper ion along the *z*-axis, see Fig. 3. In these scans, the position of the d_{xy} orbital is taken as the reference value for the d orbital energies. As expected, the energy difference $d_{xy} \rightarrow d_{x^2-y^2}$ remains constant to a good approximation, and the position of the d_{z^2} orbital is influenced significantly by the additional ligands on the *z*-axis. The energies of the d_{xz} and d_{yz} orbitals are lower in energy than the d_{xy} orbital. In the extreme case of a square planar $[Cu(NH_3)_4]^{2+}$ (Fig. 3, middle panel), the d_{z^2} orbital is found coincidentally at about the same energy as the d_{xz} and d_{yz} orbitals. Here, too, SOC does not qualitatively alter the picture, see ESI.† Tomlinson *et al.* probably investigated a mixture of structures, leading to the large line broadening of the lower intensity peak.[41] It is not possible to determine a dominant composition with the present data.

With regard to a possible ammonia π interaction, the ligand field splitting of the square planar complex can be discussed as follows. If there was no π interaction at all, the $d_{xy}(b_{2g})$ and $d_{xz/yz}(e_g)$ orbital energies ε would be degenerate (see also ESI, Fig. 3†):

$$\varepsilon_{d_{xz}} = \varepsilon_{d_{yz}} = 2e_\pi = 0$$

$$\varepsilon_{d_{xy}} = 4e_\pi = 0$$

The d_{z^2} orbital energy depends on the extent of d–s mixing, and thus could be lower or roughly equal to the energy of the aforementioned orbitals. If there is a donating π interaction, the d_{xz} and d_{yz} orbitals are shifted up by $2e_\pi$ and the d_{xy} orbital is shifted up by $4e_\pi$. Indeed, the CASSCF calculation shows that the energy of the d_{xy} orbital is significantly higher than that of the d_{yz} and d_{xz} orbitals, while the energy of the d_{z^2} orbital is accidentally equal to the ones of the d_{yz} and d_{xz} orbitals. A similar orbital energy sequence ($d_{x^2-y^2} \gg d_{xy} > d_{z^2} > d_{xz}$, d_{yz}) was assigned to the D_{4h} $[Cu(H_2O)_4]^{2+}$ subunits in meta-zeunerite $(Cu(UO_2)_2(AsO_4)_2{\cdot}8H_2O)$ by Billing *et al.*[49] For this system, a significant π interaction from the equatorial water ligands was expected.[49] Ten years later, this sequence was still considered to be plausible only for strong π donors.[50]

The energy difference between d_{xy} and d_{yz},d_{xz} from the CASSCF calculation is independent of any specific AOM fitting routine and too large to be a computational artefact. Increasing the basis set size does not lead to a qualitatively different result, see ESI.† Additionally, the computational studies mentioned above[45–48] find the same pronounced difference between the d_{xy} and d_{xz}, d_{yz} orbital energies using different levels of theory. In the AOM, the higher energy of the d_{xy} orbital can only be explained if $e_\pi > 0$. Therefore, we interpret this ligand field splitting as strong support for the existence of a π interaction for ammonia ligands.

Equilibrium AOM parameters

Having seen that a π interaction is relevant for ammonia ligands with experimental evidence and examples that do not rely on our previously introduced sampling procedure, we now

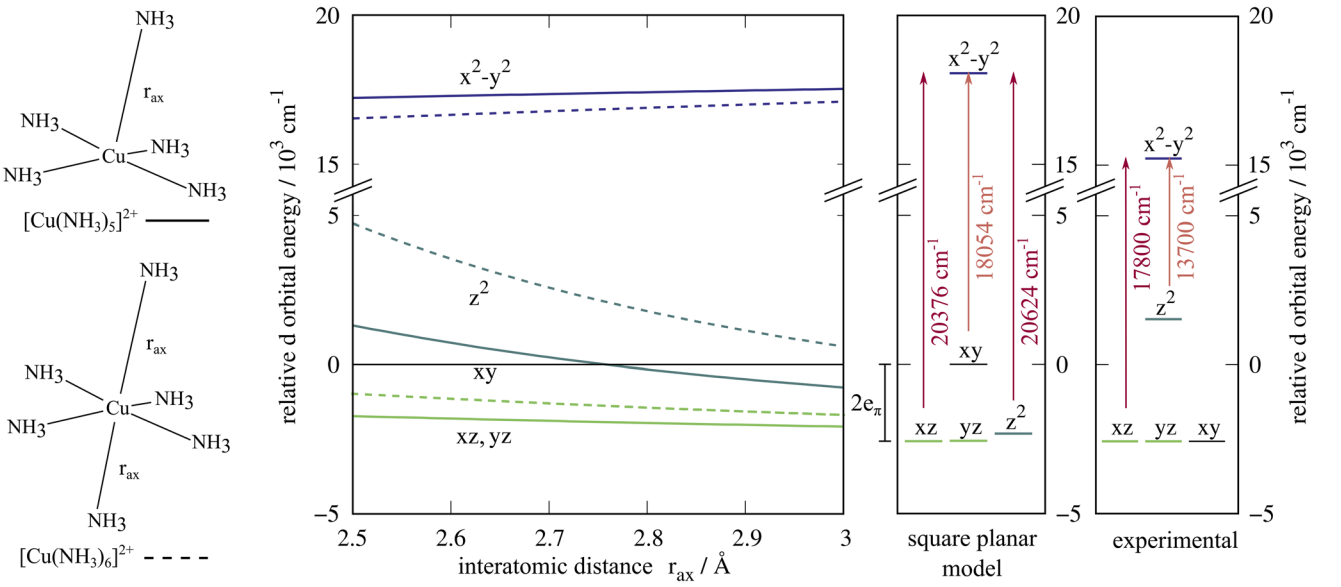

Fig. 3 Energy levels of the d orbitals in approximately square-pyramidal and octahedral ligand environments where the axial ligand positions r_{ax} are varied (left), the square planar case (middle), and the interpretation by Tomlinson, Hathaway *et al.* based on the observed UV-vis transitions (right).[41] The gaps in the crystal structure[41] might be filled with ammonia molecules, yielding a square pyramidal, elongated octahedral or square-planar case. The orbital energies are referenced to the d_{xy} orbital energy.

turn to a broader scope of complexes. Using our *ab initio* AOM sampling procedure, we evaluated a series of octahedral and tetrahedral complexes where all orbital energies affected by π interactions are degenerate so that the ammonia π interactions cannot be isolated. To this end, we chose complexes of the type $[M(NH_3)_6]^{n+}$, with M = Cr, Mn, Fe, Co, Ni, Ru, Os and n = 2, 3. We note that some of the structures are Jahn–Teller distorted and therefore have different axial and equatorial AOM parameters. For strongly distorted structures, the ligands were grouped such that those at similar bond lengths are set to have equal parameters.

The average *ab initio* AOM parameters based on CASSCF calculations are listed in Table 2 for selected equilibrium structures. Note that the standard deviations result from the data points of five distinct calculations at similar structures. While the CASSCF calculation itself may carry a systematic error that could not be avoided even with a larger number of samples, the order of magnitude was shown to be reliable.[16,18,51,52]

The *ab initio* AOM parameters identified with this procedure show a substantial π interaction for all complexes studied here. The data set is consistent with expectations and follows common trends, such as larger parameter values for higher oxidation states. Our findings for this more generalised data set thus contradict the widespread assumption of ammonia having only σ interactions.

Table 2 Ligand field parameters e_σ and e_π for complexes $[M(NH_3)_6]^{2+/3+}$ with optimized bond lengths r in Å. The multiplicity $2S + 1$ refers to the multiplicity of the optimized ground state, ΔE (kJ mol^{-1}) is the relative energy to the spin ground state structure. The ligand field parameters are calculated as averages from five asymmetric structures each; the resulting standard deviations are given in parentheses

M	$2S+1$	ΔE/kJ mol^{-1}	r/Å	e_σ/cm^{-1}	e_π/cm^{-1}
M(II)					
Mn	6	0	2.34	3613(213)	894(159)
Fe	1	5	2.05	5491(324)	710(243)
Fe	3	43	2.03^{ax}	6011(352)	1051(263)
Fe	3	43	2.25^{eq}	3772(385)	826(265)
Fe	5	0	2.28	3598(229)	851(171)
Co	4	0	2.23	3471(62)	770(19)
Co	2	7	2.39^{ax}	1818(379)	591(284)
Co	2	7	2.02^{eq}	5857(379)	1024(285)
Ni	3	0	2.18	3024(355)	412(266)
Ru	1	0	2.16	9755(203)	799(152)
Os	1	0	2.18	11 271(156)	594(120)
M(III)					
Cr	4	0	2.14	6743(341)	1027(255)
Mn	5	0	2.36^{ax}	3285(360)	576(270)
Mn	5	0	2.12^{eq}	6707(359)	1046(270)
Fe	6	56	2.23	6532(915)	2052(683)
Fe	4	47	2.32^{ax}	3909(907)	972(679)
Fe	4	47	2.08^{eq}	7452(909)	1433(682)
Fe	2	0	2.06	7042(92)	1087(74)
Co	1	0	2.02	6788(408)	698(307)
Ni	4	0	2.15^{a}	7515(1628)	1971(1238)
Ni	4	0	2.18^{b}	7500(1420)	2349(1060)
Ni	4	0	2.22^{c}	6804(1058)	2665(792)
Ru	2	0	2.16	10 749(417)	649(311)
Os	2	0	2.18	11 686(170)	194(149)

Comparison to tetrahedral complexes

To rule out any conceivable sources of error for the chemically relevant magnitude of the ammonia π interactions we have identified above, we expanded the data set to tetrahedral complexes. This tests the possibility that artefacts arise due to the overlap of two adjacent σ potentials in an octahedral, square-planar or other setting with closely spaced ligands. This overlap would occur at a position which would be covered by a π parameter. In such cases, both σ and π would be artificially increased, while the spherical contribution E would be decreased correspondingly. Therefore, it should be tested whether ammonia π parameters also appear in complexes where the ligands are spaced further apart and thus overlapping σ potentials can be ruled out.

We chose complexes of the type $[M(NH_3)_4]^{2+/3+}$ with M = Cr, Mn, Fe, Co, Ni. These complexes are hypothetical; their only purpose is to provide more room for the ligands. The fits yield *ab initio* AOM parameters that are even larger than the ones obtained for the octahedral complexes, even though some scattering is observed. We note that d–s mixing needed to be included for some of the complexes where structural deviations from ideal tetrahedral symmetry were apparent (see ESI†). In conclusion, overlapping σ potentials can be ruled out as the origin for the observed ammonia π interaction in both the octahedral and tetrahedral complexes.

Scan and comparison to halido complexes

In order to verify that the order of magnitude obtained for the ammonia π parameters is reasonable, we replaced the ammonia ligands in $[Cr(NH_3)_6]^{3+}$ with chloride ligands in exactly the same positions. Since it is widely accepted that halides and metals interact *via* a considerable π path, this data set allows a meaningful comparison with the metal–ammine parameters.

Indeed, the chloride ligands show e_π values that are even smaller than those of the ammonia ligands (e_π chloride: 313 (524) cm^{-1}, e_π ammonia: 1027(255) cm^{-1}). However, the M–NH_3 bonds in these complexes are much shorter than M–Cl bonds would be in fully relaxed complexes. For instance, the Co–NH_3 bond length in $[Co(NH_3)_6]Cl_2$ is 2.11 Å,[53] whereas the Co–Cl bond length in $CoCl_2$ is 2.51 Å.[54] The metal–chloride distance when placing the chloride ions at the nitrogen atom positions of the relaxed $[Cr(NH_3)_6]^{3+}$ complexes is thus unnaturally short, which presumably leads to the broad scattering of the parameters and the unexpectedly small e_π parameters. We observed this behaviour already in our previous study on tetrahedral halido metalates, where e_π decreases at shorter bond lengths.[16] Calculations on relaxed $[MCl_6]^{3-/4-}$ complexes yield bond lengths in the range of 2.43 Å to 2.53 Å and e_π parameters around 500 cm^{-1} with significantly less scatter (see ESI†). Scanning the metal–ligand distances in these examples from the equilibrium bond length of Cr–NH_3 to that of Cr–Cl, see Fig. 4, shows the similar order of magnitude for the e_π parameters in these two scenarios. The comparison thus confirms that the π interaction of ammonia is unlikely to be an

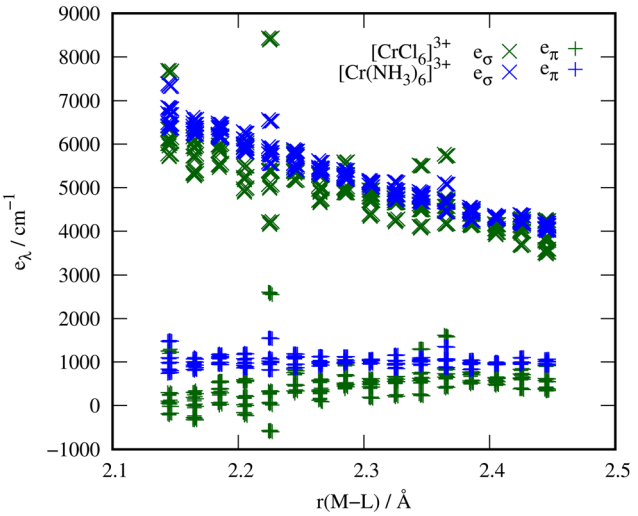

Fig. 4 Bond length scans of $[Cr(NH_3)_6]^{3+}$ and $[CrCl_6]^{3-}$ from the optimized metal–ligand bond length of the ammine complex to that of the chloride complex. The upper data points (>3000 cm^{-1}) are e_σ parameters and the lower set of data points are e_π parameters.

artefact, since the chloride interactions predicted at the same bond lengths match expectations and are qualitatively correct.

Monodentate amine ligands

To better understand the origin of the π interaction of ammonia, we studied the influence of the substituent R in $–NR_3$ on the π interaction, specifically comparing $–NH_3$ and $–NMe_3$. Complexes with different amine ligands can be compared in terms of their ligand field splitting or *via* AOM parameterization. A problem arising for such comparisons is that the bond lengths vary and hence the observed splitting is influenced by the bond length and the ligand field strength of the amine itself. While these effects cannot be disentangled fully in experimental data, it appears that the bond length is the more dominant factor in a study by Lever *et al.*[4]

Due to the bulkiness of the methylamine ligand, it is not possible to obtain reasonable structures for $[M(NMe_3)_6]^{n+}$ complexes. Therefore, we chose to study heteroleptic complexes of the type $[M(NH_3)_4(NMe_3)_2]^{n+}$, with the methylamine ligands positioned *trans* to each other, see Table 3. For all complexes, the e_σ parameters of the ammonia ligands are larger than those of the amine ligands, whereas the magnitudes of the e_π parameters are comparable or larger.

To evaluate the influence of the M–N bond length on the AOM parameters, we set the M–N bond lengths with ammonia ligands to the value of the $M–NMe_3$ distances. As expected, the e_σ and e_π parameters of the ammonia ligands decrease so that the AOM parameters of $–NMe_3$ are consistently larger than those of $–NH_3$. In the hexammine reference complex with all ammonia ligands at the same distance as the amine ligands in the relaxed structure, the ammonia ligands have very similar AOM parameters as in the mixed complex with fixed ammonia bond lengths. We can therefore conclude that amine ligands have intrinsically higher e_π parameters than ammonia ligands. This comparison furthermore points towards hyperconjugation of the N–R bonds as a possible origin of the π interaction for both amines and ammonia.

From a molecular orbital perspective, the chemical origin and a possible explanation for the considerable π interaction of ammonia ligands may lie in the hyperconjugation of the N–H bonds with the respective d orbitals. Hyperconjugation was already observed and interpreted by Mulliken[55–57] and became an important tool for rationalizing formation and stabilization energies[58] and chemical shifts in NMR experiments.[59]

Table 3 AOM parameters (cm^{-1}) of complexes of the type $[MA_4B_2]^{n+}$ and $[MA_6]^{n+}$ with A = NH_3 and B = NMe_3. The methylamine ligands are placed trans to each other. The bond lengths *r*(M–L) (Å) are shown for each ligand type. For each metal ion, three sets of parameters are given: one for the fully optimized structure at the multiplicity indicated with a superscript, one for a structure where the equatorial $M–NH_3$ bonds are set to the optimized $M–NMe_3$ bond length,[a] and one for a reference hexammine complex where all $M–NH_3$ bonds are fixed at this value[b]

Complex		A = NH_3			B = NMe_3		
Composition	Bond lengths	*r*(M–L)/Å	e_σ/cm^{-1}	e_π/cm^{-1}	*r*(M–L)/Å	e_σ/cm^{-1}	e_π/cm^{-1}
$^4[CrA_4B_2]^{3+}$	Optimized	2.13	8115(842)	1944(632)	2.34	6291(847)	1917(634)
$[CrA_4B_2]^{3+}$	Fixed	2.34	5228(222)	1378(167)	2.34	6425(223)	1746(167)
$[CrA_6]^{3+}$	Fixed	2.34	5143(93)	1193(71)			
$^6[MnA_4B_2]^{2+}$	Optimized	2.33	3946(247)	1023(185)	2.53	2793(247)	905(185)
$[MnA_4B_2]^{2+}$	Fixed	2.53	2667(63)	866(47)	2.53	2992(63)	975(47)
$[MnA_6]^{2+}$	Fixed	2.53	2667(21)	849(17)			
$^5[FeA_4B_2]^{2+}$	Optimized	2.25	4740(185)	1548(137)	2.48	3360(185)	1410(138)
$[FeA_4B_2]^{2+}$	Fixed	2.48	2981(104)	1152(77)	2.48	3320(106)	1268(79)
$[FeA_6]^{2+}$	Fixed	2.48	2864(64)	1044(47)			
$^1[CoA_4B_2]^{3+}$	Optimized	2.00	8353(623)	1518(469)	2.29	5018(636)	1290(471)
$[CoA_4B_2]^{3+}$	Fixed	2.29	4439(38)	992(28)	2.29	6032(39)	1365(29)
$[CoA_6]^{3+}$	Fixed	2.29	4531(84)	853(63)			

[a] The NH_3 ligands were moved with no subsequent geometry optimization. [b] The NMe_3 ligands were replaced with NH_3 with subsequent optimization of the positions of the new hydrogen atoms.

Experimental NMR studies of $Ru(NH_3)_x$ complexes show that there is an interaction between N–H bonds and the metal d orbitals, leading to measurable hyperfine interactions. This interaction is explained by hyperconjugation of the N–H bonding orbital with the ruthenium d orbital.[60–62]

An alternative view is offered by the interpretation of ligand field splittings in terms of electrostatic potentials as developed by Gerloch and Woolley.[63–65] This picture is completely independent of molecular orbital theory and treats the influence of the ligands on the d orbital energies purely electrostatically. With this approach, the π interaction could be explained by the electron density of the N–H bond and the negative partial charge on the nitrogen atom exerting an influence on the metal d orbital energies.

Both interpretations are supported by the results for the methylamine complexes. The larger N–C bonding orbital of $–NMe_3$ compared to the N–H bonding orbitals of $–NH_3$ suggest a stronger hyperconjugation with the metal d orbitals. Likewise, the methyl groups are electron donating, leaving a higher electron density at the nitrogen and thus supporting the picture of an electrostatic ligand field interaction.

Chelating amine ligands

When applying the aiLFT procedure on ethylenediamine (en) and diethylenetriamine (dien), it is apparent that it is not possible to obtain a good fit to the d orbital energies with just e_σ and e_π. We attribute this to an effect called "misdirected valency" by Deeth *et al.*[48,66–69] Misdirected valency is caused by bent bonding and non-bonding lone pairs where the centroid of the bond is not aligned with the metal–ligand axis, as depicted in ref. 66. For the chelating en and dien ligands, the M–N bond is bent because of the orientation of the carbon backbone. We note that methylamine, although not chelating, also shows slight off-axis bonding since the bulky $–CH_3$ groups prevent full alignment. The parameters found for chelating amines (shown in the ESI†) should therefore be interpreted with some caution.

If the metal–ligand interaction is asymmetric with respect to the bonding axis, it cannot be fully described by the set of parameters employed. It is in principle possible to include off-diagonal $e_{\sigma\pi}$ parameters in the AOM parameterisation.[48] Naturally, this would aggravate the underdetermination problem and hinder a clear interpretation of the results.

Conclusions

To summarise, we presented indications that the widespread assumption of ammonia being a σ-only ligand might be incorrect. Our findings question the reliability of published AOM parameters for ammonia complexes from previous fitting procedures applied to experimental and computational data where e_π was neglected, noting of course that this was often done to reduce the number of AOM parameters. Without this assumption, many cases would not have been solvable. Our work furthermore raises the question whether any ligand can be considered a σ-only ligand.

Conflicts of interest

There are no conflicts to declare.

Acknowledgements

The authors thank R. J. Deeth for many fruitful discussions and valuable input. The reviewers' comments were greatly appreciated. This work was funded by the Deutsche Forschungsgemeinschaft (DFG, German Research Foundation) – CRC 1487, "Iron, upgraded!" – project number 443703006.

References

1 D. W. Smith, *J. Chem. Soc. A*, 1969, 1708–1712.
2 C. E. Schäffer, *Pure Appl. Chem.*, 1970, **24**, 361–392.
3 M. Gerloch, J. H. Harding and R. G. Woolley, *Inorganic Chemistry*, Berlin, Heidelberg, 1981, pp. 1–46.
4 A. B. P. Lever, I. M. Walker, P. J. McCarthy, K. B. Mertes, A. Jircitano and R. Sheldon, *Inorg. Chem.*, 1983, **22**, 2252–2258.
5 R. J. Deeth and M. Gerloch, *Inorg. Chem.*, 1984, **23**, 3846–3853.
6 M. Sano, T. Maruo, Y. Masuda and H. Yamatera, *Inorg. Chem.*, 1984, **23**, 4466–4469.
7 A. Bencini, C. Benelli and D. Gatteschi, *Coord. Chem. Rev.*, 1984, **60**, 131–169.
8 P. V. Bernhardt and P. Comba, *Inorg. Chem.*, 1993, **32**, 2798–2803.
9 T. Schönherr, M. Itoh and A. Urushiyama, *Bull. Chem. Soc. Jpn.*, 1995, **68**, 2271–2276.
10 M. Atanasov, P. Comba, S. Helmle, D. Müller and F. Neese, *Inorg. Chem.*, 2012, **51**, 12324–12335.
11 D. Schweinfurth, M. G. Sommer, M. Atanasov, S. Demeshko, S. Hohloch, F. Meyer, F. Neese and B. Sarkar, *J. Am. Chem. Soc.*, 2015, **137**, 1993–2005.
12 P. Comba, G. Nunn, F. Scherz and P. H. Walton, *Faraday Discuss.*, 2022, **234**, 232–244.
13 C. E. Schäffer and C. K. Jørgensen, *Mol. Phys.*, 1965, **9**, 401–412.
14 M. Suta, F. Cimpoesu and W. Urland, *Coord. Chem. Rev.*, 2021, **441**, 213981.
15 B. N. Figgis and M. A. Hitchman, *Ligand Field Theory and Its Applications*, Wiley-VCH, New York, 1st edn, 2000.
16 M. Buchhorn, R. J. Deeth and V. Krewald, *Chem. – Eur. J.*, 2022, **28**, e202103775.
17 M. Atanasov, D. Ganyushin, K. Sivalingam and F. Neese, *Molecular Electronic Structures of Transition Metal Complexes II*, Springer Berlin/Heidelberg, Berlin, Heidelberg, 2011/2012, pp. 149–220.

18 J. Jung, M. Atanasov and F. Neese, *Inorg. Chem.*, 2017, **56**, 8802–8816.
19 S. K. Singh, J. Eng, M. Atanasov and F. Neese, *Coord. Chem. Rev.*, 2017, **344**, 2–25.
20 F. Neese, *Wiley Interdiscip. Rev.: Comput. Mol. Sci.*, 2012, **2**, 73–78.
21 F. Neese, *Wiley Interdiscip. Rev.: Comput. Mol. Sci.*, 2018, **8**, e1327.
22 A. D. Becke, *Phys. Rev. A*, 1988, **38**, 3098–3100.
23 J. P. Perdew, *Phys. Rev. B: Condens. Matter Mater. Phys.*, 1986, **33**, 8822–8824.
24 F. Weigend and R. Ahlrichs, *Phys. Chem. Chem. Phys.*, 2005, **7**, 3297.
25 F. Weigend, *Phys. Chem. Chem. Phys.*, 2006, **8**, 1057–1065.
26 E. J. Baerends, D. E. Ellis and P. Ros, *Chem. Phys.*, 1973, **2**, 41–51.
27 O. Vahtras, J. Almlöf and M. W. Feyereisen, *Chem. Phys. Lett.*, 1993, **213**, 514–518.
28 V. Barone and M. Cossi, *J. Phys. Chem. A*, 1998, **102**, 1995–2001.
29 A. V. Marenich, C. J. Cramer and D. G. Truhlar, *J. Phys. Chem. B*, 2009, **113**, 6378–6396.
30 P. Siegbahn, A. Heiberg, B. Roos and B. Levy, *Phys. Scr.*, 1980, **21**, 323–327.
31 B. O. Roos, P. R. Taylor and P. E. Siegbahn, *Chem. Phys.*, 1980, **48**, 157–173.
32 C. Angeli, R. Cimiraglia and J.-P. Malrieu, *Chem. Phys. Lett.*, 2001, **350**, 297–305.
33 C. Angeli, R. Cimiraglia, S. Evangelisti, T. Leininger and J.-P. Malrieu, *J. Chem. Phys.*, 2001, **114**, 10252–10264.
34 C. Angeli, R. Cimiraglia and J.-P. Malrieu, *J. Chem. Phys.*, 2002, **117**, 9138–9153.
35 C. Angeli and R. Cimiraglia, *Theor. Chem. Acc.*, 2002, **107**, 313–317.
36 F. Neese, *J. Chem. Phys.*, 2005, **122**, 34107.
37 R. G. Woolley, *Mol. Phys.*, 1981, **42**, 703–720.
38 M. Duggan, N. Ray, B. Hathaway, G. Tomlinson, P. Brint and K. Pelin, *J. Chem. Soc., Dalton Trans.*, 1980, 1342.
39 B. J. Hathaway and A. Tomlinson, *Coord. Chem. Rev.*, 1970, **5**, 1–43.
40 R. J. Deeth and C. M. Kemp, *J. Chem. Soc., Dalton Trans.*, 1992, 2013–2017.
41 A. A. G. Tomlinson, B. J. Hathaway, D. E. Billing and P. Nichols, *J. Chem. Soc. A*, 1969, 65.
42 A. Ferrari, A. Braibanti and A. Tiripicchio, *Acta Crystallogr.*, 1966, **21**, 605–610.
43 B. Morosin and A. C. Larson, *Acta Crystallogr., Sect. B: Struct. Crystallogr. Cryst. Chem.*, 1969, **25**, 1417–1419.
44 B. J. Hathaway and F. Stephens, *J. Chem. Soc. A*, 1970, 884.
45 F. Neese, *Magn. Reson. Chem.*, 2004, **42**, 187–198.
46 S. Vancoillie and K. Pierloot, *J. Phys. Chem. A*, 2008, **112**, 4011–4019.
47 E. Giner, D. P. Tew, Y. Garniron and A. Alavi, *J. Chem. Theory Comput.*, 2018, **14**, 6240–6252.
48 M. Atanasov, P. Comba, C. A. Daul and F. Neese, *Models, mysteries, and magic of molecules*, Springer, Dordrecht, The Netherlands, 2008, pp. 411–445.
49 D. E. Billing, B. J. Hathaway and P. Nicholls, *J. Chem. Soc. A*, 1969, 316.
50 Y. Nishida and S. Kida, *Coord. Chem. Rev.*, 1979, **27**, 275–298.
51 D. Aravena, M. Atanasov and F. Neese, *Inorg. Chem.*, 2016, **55**, 4457–4469.
52 L. Lang, M. Atanasov and F. Neese, *J. Phys. Chem. A*, 2020, **124**, 1025–1037.
53 M. T. Barnet, B. M. Craven, H. C. Freeman, N. E. Kime and J. A. Ibers, *Chem. Commun.*, 1966, 307–308.
54 H. Grime and J. A. Santos, *Z. Kristallogr. - Cryst. Mater.*, 1934, **88**, 136–141.
55 R. S. Mulliken, *Phys. Rev.*, 1933, **43**, 279–302.
56 R. S. Mulliken, *J. Chem. Phys.*, 1939, **7**, 339–352.
57 R. S. Mulliken, C. A. Rieke and W. G. Brown, *J. Am. Chem. Soc.*, 1941, **63**, 41–56.
58 J. I.-C. Wu and P. v. R. Schleyer, *Pure Appl. Chem.*, 2013, **85**, 921–940.
59 J. W. de M. Carneiro, J. F. Dias, J. G. R. Tostes, P. R. Seidl and C. A. Taft, *Int. J. Quantum Chem.*, 2003, **95**, 322–328.
60 M. L. Naklicki, C. A. White, V. V. Kondratiev and R. J. Crutchleya, *Inorg. Chim. Acta*, 1996, **242**, 63–69.
61 B. R. McGarvey, N. C. Batista, C. W. B. Bezerra, M. S. Schultz and D. W. Franco, *Inorg. Chem.*, 1998, **37**, 2865–2872.
62 W. M. Laidlaw, R. G. Denning, J. C. Green, J. Boyd, J. Harmer and A. L. Thompson, *Inorg. Chem.*, 2013, **52**, 7280–7294.
63 R. J. Deeth and M. Gerloch, *J. Chem. Soc., Dalton Trans.*, 1986, 1531–1534.
64 R. G. Woolley, *Int. Rev. Phys. Chem.*, 1987, **6**, 93–141.
65 M. Gerloch, *Understanding Molecular Properties*, D. Reidel Publishing Company, Dordrecht, 1987, pp. 111–142.
66 R. J. Deeth, M. J. Duer and M. Gerloch, *Inorg. Chem.*, 1987, **26**, 2573–2578.
67 R. J. Deeth, M. J. Duer and M. Gerloch, *Inorg. Chem.*, 1987, **26**, 2578–2582.
68 R. J. Deeth and M. Gerloch, *Inorg. Chem.*, 1987, **26**, 2582–2585.
69 M. J. Duer, N. D. Fenton and M. Gerloch, *Int. Rev. Phys. Chem.*, 1990, **9**, 227–280.